UNITÉ DE RECHERCHE
INRIA-ROCQUENCOURT

Institut National
de Recherche
en Informatique
et en Automatique

Domaine de Voluceau
Rocquencourt
B.P.105
78153 Le Chesnay Cedex
France
Tél.:(1) 39 63 55 11

Rapports de Recherche

N° 1388

Programme 6
Calcul scientifique, Modélisation et
Logiciels numériques

A MULTIRESOLUTION METHOD FOR DISTRIBUTED PARAMETER ESTIMATIONS

Jun LIU

Janvier 1991

RR-1388

A Multiresolution Method For Distributed Parameter Estimations

Méthode Multirésolution Pour L'estimation des Paramètres Répartis

Jun Liu

Ident Project, INRIA, Rocquencourt
78153 Le Chesnay, France.

February 6, 1991

Abstract

A multiresolution method for the resolution of distributed parameter estimation (inverse problem) is studied numerically We consider the identification of the coefficient of an elliptic equation in one dimension as our model problem. First, we use multiscale bases to analyze the degree of ill-posedness of the inverse problem. Secondly, we show that the method of scale by scale multiresolution yields robust and fast convergence. Finally, we show how the method gives a natural regularization approach which is complementary to Tikonov's regularization.

Keywords

identification, distributed parameter, multiresolution, Haar basis, BFGS optimization

Résumé

Une méthode multirésolution pour l'estimation des paramètres répartis (problème inverse) est étudiée du point de vue numérique. Le problème modèle considéré est l'identification d'un coefficient dans une équation elliptique de dimension un. On utilise d'abord des bases multi-échelles pour analyzer le degré de la non linéarité du problème inverse. Ensuite, on montre que la methode de multirésolution échelle par échelle produit une convergence robuste et rapide. Enfin, on montre comment la méthode donne une approche naturelle de régularisation qui est complémentaire de la régularisation de Tikonov.

Mots-Clé

identification, paramètre réparti, multirésolution, base de Haar, optimisation BFGS

Contents

I Introduction

Inverse problems are usually considered as difficult problems. One essential question is how to obtain rapidly a stable solution. The idea of multiscale representation has suggested various parallel and iterative algorithms. For example, multigrid methods have been widely used for solving partial differential equations (direct problems) [4, 5] in order to accelerate the convergence. However, this idea has been rarely used until now for inverse problems (lack of theory). Recently, some approximation framework have been developed for inverse problems [2] and wavelet theory (multiscale bases) have appeared [14, 13]. This allows the idea of multiresolution to be used for inverse problem without grand modification from the classical optimization methods.

We take a simple elliptic problem as our model problem, which is a well known nonlinear ill-posed problem. A number of study for this problem have been done (for example [12]). In this paper, we first analyze the inverse problem using the Haar basis (a multiscale basis). We remark that the objective function is more "ill-posed" (or nonlinear) with respect to the coefficients corresponding to the finer scales, but it is less sensible with respect to these coefficients. Then we investigate numerically the behavior of a BFGS optimization routine in the IMSL library [11] when the unknown parameter is represented on the usual local basis, and on the Haar basis. This leads us to propose a multiresolution, or scale by scale, optimization method to solve the parameter estimation problem. This method turns out to be very robust (convergence is obtained for any initialization of the optimization algorithm) and efficient (a good solution is obtained in a very small number of iterations). The multiresolution method allows, for the problem under consideration, to perform a global optimization with a local optimizer. Finally we give regularization methods which are complementary to Tikonov's regularization. A number of numerical results are shown.

II A simple model inverse problem

We consider the following elliptic equation:

$$-\frac{d}{dx}(a(x)\frac{du(x)}{dx}) = f(x) \qquad x \in (0,1) \tag{1}$$

with the Dirichlet's boundary condition:

$$u(0) = u(1) = 0. \tag{2}$$

where $f(x) \in L^2(0,1)$ is known.

The direct problem is:

(DP) let Q_{ad} be the convex set $\{a(x) \mid 0 \leq m \leq a(x) \leq M \ , x \in (0,1)\} \subset L^\infty$; given $a(x) \in Q_{ad}$, we solve for $u(x)$ in the equations (1),(2).

This problem is very simple, as the equations (1),(2) have a unique solution $u(x)$ denoted by $\Phi(a)$. The application Φ is continue from Q_{ad} equipped with the L^∞-norm into $H_0^1 \subset L^2$.

The inverse problem is:

(IP) given a distributed observation $z(x) \in L^2(0,1)$ of $u(x)$, we minimize the objective function (output least square error):

$$J(a) = \|\Phi(a) - z\|^2 = \int_0^1 (u(x) - z(x))^2 dx \tag{3}$$

over $a \in Q_{ad}$.

The problem is a typical ill-posed nonlinear problem. There are two types of "ill-posedness". First $a(x)$ cannot be determined by equation (1) on the set $\{x|u_x(x) = 0\}$ so that there is no uniqueness for the solution if $measure(\{x|u_x(x) = 0\}) > 0$. Secondly, from homogenization theory [3], we remark that there is a sequence of $a_n(x)$ which is not convergent in L^∞, but still the sequence $u_n(x) = \Phi(a_n(x))$ is convergent in $H_0^1(0,1)$, so that the solution is not stable.

Remark: we can obtain easily an analytical solution of equation (1),(2):

$$u(x) = \frac{\int_0^1 b(y)F(y)dy \int_0^x b(y)dy}{\int_0^1 b(y)dy} - \int_0^x b(y)F(y)dy \tag{4}$$

with

$$b(x) = a(x)^{-1}, \ F(y) = \int_0^y f(s)ds \tag{5}$$

This analytical solution will be used in paragraph 3.2.

For the numerical solution of (IP), we shall consider the following discretized problem (IP_h^H):

$$Minimize \quad J_h(a_H) = \sum (u_h - z_h)^2 \tag{6}$$

with

$$A_h(a_H)u_h = f_h, \tag{7}$$

where u_h and a_H are the discretization of $u(x)$ and $a(x)$ respectively ($h = 1/n$ and $H = 1/N$): u_h is made of the $n-1$ values of u_h at the nodes $x_i = ih$, $i = 1, ..., n-1$ and a_H is made of the N values of a_H on intervals $](i-1)H, iH[$, $i = 1, 2, ..., N$.

Remark: for well-posedness of the discrete problem (IP_h^H), the condition $h \leq H$ is necessary. When $H = h$, we have $N = 1/H$ numbers to be estimated, but only $N-1$ observation numbers.

III Using multiscale bases to analyze the inverse problem

III-1 Multiscale Bases

Multiscale bases exist since a very long time, the first one being the Haar basis which appeared at the beginning of this century. They were however relatively little used for numerical computations, until the uproar around the wavelets which developed in the early 80's. Presented first as a challenge to Fourier Analysis, the wavelets turned out quickly to be a systematical way of constructing multiscale basis of function spaces. The use of these multiscale bases is now being widely investigated for the resolution of partial differential equations (Direct Problem). We show in this paper that they can be a very valuable (and simple) tool for the resolution of the inverse problem stated in paragraphe 2. Because the parameter $a(x)$ we are looking for is required only to be in $L^2(0,1)$, we shall use the simplest multiscale basis, namely the Haar basis. Of course, in inverse problems where the unknown parameter is more regular, we will have to resort to more sophisticated wavelet bases.

Let Z be the set of relative integer, using the characteristic function

$$\phi(x) = \begin{cases} 1 & x \in (0,1) \\ 0 & otherwise, \end{cases}$$

the mth scale approximation of a general function $a(x)$ is represented by

$$a^m(x) = \sum_{i \in Z} a_i^m \phi(2^m x - i) \tag{8}$$

where a_i^m is the mean values of $a(x)$ over the interval $[i/2^m, (i+1)/2^m]$.

The corresponding multiscale basis is the Haar basis, made of the functions $\psi_i^j(x) = \psi(2^i x - j)$ for all $i, j \in Z$, which are constructed from the following mother wavelet function:

$$\psi(x) = \begin{cases} -1 & x \in (0,1/2) \\ +1 & x \in (1/2,1) \\ 0 & otherwise. \end{cases}$$

The ψ_i^j, $i, j \in Z$ form a complete orthogonal basis of $L^2(R)$, which is multiscale in the sense that the mth scale approximation $a^m(x)$ is simply obtained by setting to zero all coefficients of ψ_i^j with $j \geq m$ in the expansion of the function

$$a(x) = \sum_{i \in Z, j \in Z} c_i^j \psi_i^j(x) \tag{9}$$

on the basis.

Remark: for the space $L^2(0,1)$ and a fixed mth scale approximation, we have two equivalent orthogonal bases: the characteristic basis made of $\{\phi(2^m x - i + 1) |\ i = 1, ..., 2^m\}$ and the Haar basis made of $\{\psi(2^j x - i + 1) |\ j = 0, ..., m-1, i = 1, ..., 2^j\}$ and of the constant function $\psi^0(x) = \phi(x) = 1$ over [0,1].

III-2 Curvature's Analysis

A geometrical theory for general nonlinear least-square problems [7] shows that the velocity and the curvature along curves of the solution space which are images by Φ of segments of Q_{ad} are important to measure the "degree of ill-posedness" of the inverse problem with output least-square formulation. In the limiting case, the curvature is equal to zero for a linear problem.

In this section, we suppose $f(x) = 1$. The algebraic computation systems (Macsyma, Maple etc) allow us to calculate the velocity and the curvature along the curve $\Phi(a + t\delta a)$ at $t = 0$ for the directions of the base functions:

$$\delta a(x) = \begin{cases} 0 & x \in (0, t-h) \\ -1 & x \in (t-h, t) \\ 1 & x \in (t, t+h) \\ 0 & x \in (t+h, 1), \end{cases}$$

for the exact mapping Φ, i.e. without any approximation to the solution $u(x)$ of equations (1) and (2).

We obtain for the velocity V and the curvature K in the direction $\delta a(x)$ at $a(x) = 1$ the following formulae:

$$V^2 = \frac{h^3(180hs^2 + 5h + 30h^3 + 40s^2 - 24h^2)}{60} \tag{10}$$

$$\begin{aligned} K^2 = & \\ & -480(1230h^7 - 600h^8 - 940h^6 + 317h^5 - 40h^4 + 1800h^7s^2 - 400s^4 \\ & -3000h^6s^2 + 7200h^4s^4 + 2640h^4s^2 + 480h^2s^4 + 240h^2s^2 \\ & -1480h^3s^2 - 8400h^3s^4 - 330h^5s^2 + 7200hs^6 + 1600hs^4 - 4800s^6) \\ & (180hs^2 + 5h + 30h^3 + 40s^2 - 24h^2)^{-3}h^{-4} \end{aligned} \tag{11}$$

where $s = t - 1/2$.
From these formulae, we have

$$V^2 \sim \frac{2h^3s^2}{3}, \qquad K \sim 6h^{-2} \qquad as \quad h \sim 0 \tag{12}$$

The conclusion is that the objective function is more nonlinear with respect to the coefficients of the finer scales, but is less sensitive with respect to these coefficients. For illustration, we plot the curves $log(V)$ and $log(1 + K^2)$ at five different scales in Figure 1 (bottom).

Remark: In the same way, we have for the characteristic basis:

$$V^2 = \frac{h^2(h^3 + 30h^2s^2 - 20hs^2 + 10s^2 + 120s^4)}{120} \tag{13}$$

$$K^2 = -\frac{4800h^3s^2(10hs^2 + 2h - 12s^2 - 1 - h^2)}{(h^3 + 30h^2s^2 - 20hs^2 + 10s^2 + 120s^4)^3} \tag{14}$$

$$V^2 \sim \frac{h^2 s^2(1+12s^2)}{12}, \quad K^2 \sim \frac{4.8h^3}{s^4(1+12s^2)^2} \quad as \quad h \sim 0 \qquad (15)$$

in the direction of the base function:

$$\delta a(x) = \begin{cases} 0 & x \in (0, t-h/2) \\ 1 & x \in (t-h/2, t+h/2) \\ 0 & x \in (t+h/2, 1) \end{cases}$$

where $s = t - 1/2$.

Remark: If we take $b(x) = a(x)^{-1}$ as the parameter to be estimated, we have not the same result. The curvature K in the direction $\delta b(x)$ at $b(x) = 1$ is the following:

$$K^2 = \frac{9600h^2(5-24h+60s^2+30h^2-90hs^2)}{(5h+40s^2-24h^2+180hs^2+30h^3)^3} \qquad (16)$$

$$K^2 \sim \frac{3h^2(1+12s^2)}{4s^6} \qquad as \quad h \to 0 \qquad (17)$$

where $s = t - 1/2$ and

$$\delta b(x) = \begin{cases} 0 & x \in (0, t-h) \\ -1 & x \in (t-h, t) \\ 1 & x \in (t, t+h) \\ 0 & x \in (t+h, 1) \end{cases}$$

It is not surprising that the equations (12), (15), (17) are very different. The equation (12) show that singularity directions for $K = \infty$ correspond to $h = 0$ and from the equations (15), (17) singularity directions for $K = \infty$ correspond to $s = 0$. These two kinds of singularity directions correspond to exactly the two kinds of ill-posedness mentioned in the paragraph 2.

IV Multiscale parametrization, Multiresolution and Regularization

We investigate in this paragraph various strategies for the practical computation of a_H by minimization of the objective function J_h. We have used in all runs the subroutine BCONF of the IMSL library based on the BFGS algorithm [11]. The only initializations required in this subroutine are the

initial guess of the unknown parameter and the other parameters are given by default values (the initialization of the Hessian is an identical matrix).

Our investigations concerned first the behavior of the BFGS algorithm for various initializations and various parametrizations of a_H associated to different bases of R^{32}: the characteristic (or local) basis (the paragraph IV-1) and multiscale bases (the paragraph IV-2). Parametrization on the usual Haar basis will prove to yield in many case a much better convergence of the BFGS algorithm than the usual local basis.

Our analysis of this phenomenon will lead us to experiment with a multiresolution (scale by scale) optimization approach in the paragraph IV-3, which turns out to be very robust and yields the fastest convergence. Finally, we show in the paragraph IV-4 how multiscale parametrization and multiresolution can be efficiently combined with a regularization approach in order to stabilize the estimation of a_H with noisy data.

We summarize here the data common to all runs: the elliptic equation (1),(2) (with right hand side $f(x) = 1$) was discretized using a finite difference scheme with a mesh size $h = 1/32$, and the parameter a_H was also discretized with $H = 1/32$ (hence we are faced with the estimation of 32 unknown parameters).

The data z_h (exact in the sections IV-1, IV-2 and IV-3 as well as noisy in the section IV-4) was generated using the above finite difference scheme and the following "true parameter"

$$a_H^{true}(x) = \begin{cases} 1 & x \in (0, 1/5) \\ 10 & x \in (1/5, 2/3) \\ 50 & x \in (2/3, 1). \end{cases}$$

Notice that a_H^{true} is quite strongly heterogeneous ! Because of the Dirichlet boundary condition, z_h consisted only in 31 numbers representing the solution $u(x)$ at $x = h/2, 3h/2, ..., 63h/2$. Hence the problem of the estimation of a_H from z_h was clearly undetermined !

Two initializations were used, corresponding to $a_H^{init} = 1$ and 10. The first initial guess is "poor" (underestimated), and the second one is a "good" one (in the range of the values of a_H^{true}). The corresponding initial values of J_h are 215. and 0.84 respectively. Optimization runs using the local basis

were made with the bound constraint of $0.1 \leq a_H \leq 100$. (except one run in paragraph 4.2) and optimization runs using the multiscale basis or using the multiresolution method were performed without any constraint.

IV-1 The BFGS algorithm and the local basis

The traditional method is to perform one optimization run to estimate simultaneously 32 numbers representing the value of a_H on each interval. If we use the subroutine BCONF in this way, we obtain the result shown at bottom left of Figure 2 after 1000 iterations with initialization $a_H^{init} = 1$. The algorithm is not convergent and final relative objective function is equal to 3.0e-4. If we choose the better initialization $a_H^{init} = 10$, we obtain the result shown at top left of Figure 2. We have recoved the "true" parameter a_H^{true}, but the rate of convergence is slow. To understand in more details the behavior of the algorithm on the problem, we plot the evolution of the relative errors for parameter at different scales in L^2 during the procedure of optimization in Figure 3, 4. The result coincides with the analysis in paragraph 3. The coefficients of finer scales do not converge toward the "true" coefficients at all when the "bad" initialization $a_H^{init} = 1$ is used.

IV-2 The BFGS algorithm and Multiscale bases

We tested the influence of the representation of a_H on the Haar basis (orthogonal) as in (9), on the normalized Haar basis (orthonormal) and on the local basis (orthonormal) when a minimization without constraint was performed for the three bases. Notice that quasi-Newton algorithm are expected to produce the same sequence of iterates when an orthonormal change of basis is performed on the unknown parameter and when the Hessian is initialized with an identity matrix in both cases. Hence one expects that using the local basis or the normalized Haar basis will not influence on the behavior of the BFGS algorithm. This is what we observe on figure 5. However, the decrease of the objective function is slightly better with the normalized Haar basis for the two initializations $a_H^{init} = 1$ and $a_H^{init} = 10$.

Then we used the usual Haar basis for the parametrization of the unknown parameter a_H . As we already noticed in [8], the convergence of the BFGS algorithm was much better with this basis for the two initializations $a_H^{init} = 1$ and $a_H^{init} = 10$ (figure 5). We try now to give an explanation of this phenomenon. We notice first that in the Haar basis, the L^2-norm of the basis

function is decreasing when the scale index is increasing. Hence replacing the local or normalized Haar basis by the Haar basis amounts to perform a rescaling of the unknown parameter depending on the scale level: the sensitivity to an unknown is decreased proportionally to his scale index (this is apparent by comparing the top and bottom of left part of figure 1). Surprisely at first glance, this rescaling goes in the opposite direction of what would be required to try to "spherize' the objective function J_h around its minimum: the discrepancy in sensitivity in all basis directions is much larger with the Haar basis (bottom left of figure 1) than with the normalized Haar basis (top left of figure 1)! Numerical experimentation with an "overnormalized" Haar basis (for which all scale had approximately the same sensitivity) did not produce any enhancement of the convergence.

The explanation may come from the nonlinear effects: as we already mentioned it in paragraph 3.2, the non linearity is increasing with the scale index, hence "spherizing" the objective function, which requires to boost up the sensitivity of fine (high index) scales, also boosts up the nonlinear effects associated to these fine scale, so that the "convergence domain" around the exact solution becomes extremely small, and the quasi-Newton method is not able to find its way to the global minimum as soon as the initial guess is not too good. Conversely "despherizing" the objective function, i.e. still diminishing the sensitivity of fine (high index) scales (which is performed by using the Haar basis), also lowers the influence of the strong non linearities associated to fine scales coefficients: at the beginning the objective function seems to depend almost only on the low scales, low nonlinear coefficients. It is only once these low scales coefficients have been approximately set that the influence of the finer scale coefficients become apparent. This is confirmed on figures 6 and 7, where the evolution of the relative errors on a_H is plotted for each scale against the iteration index. On figure 6 for example, we see that coefficients associated to scales 1 and 2 begin to adjust only after iteration 20, when the scale zero (mean value) coefficient has been approximated to 10%. Similarly, until iteration 150, the BFGS algorithm basically don't touch the coefficient of the finer scales ($3th$, $4th$ and $5th$), and hence performs an optimization in the 4 dimension space associated to scale 0, 1 and 2 ! Also, one sees that the coefficients of the finest ($5th$) scale begin to really adjust only after iteration 340, where the error on all coarser scales becomes below 10% !

This behavior suggests strongly to try to optimize the objective function

successively on spaces of increasing dimensions associated to finer and finer scales. This is the subject of the next paragraph.

IV-3 Multiresolution algorithms

As we have seen above, the nonlinear effects are increasing when finer scales are added, and the size of the corresponding "domain of convergence" of the quasi-Newton method is decreasing. It is hence natural to solve first the optimization problem on a small number of (coarser) scales which is likely to yield the global minimum as the nonlinear effects are small, and to use this point as initial guess for an optimization run including more scale index. The hope being this initial guess will be inside the "convergence domain" of the new, more nonlinear problem. This is the basis of the multiresolution algorithm.

Another argument is the estimation of approximation error. In the solution of the PDE (direct problem), we have the following error estimation [1, 9]:

$$\|u_h - u\| \leq K h^\alpha \tag{18}$$

This error estimation is usually considered as an essential support for the full multigrid methods (nested algorithm) [5]. For inverse problems, an approximation theory have been also developed recently for elliptic problem in some special case [2, 10] under the condition $h \sim H$, which gives for non noisy data a similar estimation:

$$\|a_H - a\| \leq K_2 H^\beta \tag{19}$$

This also suggests to use a nested algorithm for our inverse problem.

The multiresolution algorithm is as follows: we solve first the optimization problem with scale zero (one unknown), the result is used as initial value for an optimization run with scale one (two unknowns) etc. This algorithm can be implemented using either the local basis or the Haar basis. The advantage of the local basis is to allow for an easy implementation of the bound constraint, but our numerical experiments show that with multiresolution algorithm the solution does not tend to hit the constraints. The multiscale basis allows to perform easily multigrid patterns as V, W cycles. But the inverse problem has not the same behavior as the direct problem and until now we have not found any need of using such patterns. We illustrate on figures 8, 9 and 10 the behavior of local basis implementation of the

multiresolution algorithm. Figure 8 shows that multiresolution achieves an excellent fit (objective function =1.e-10) in only 120 iterations, and beats clearly (mono)resolution with either local or Haar basis (compare also with figure 5). The figure 9 shows the parameter obtained at the end of each of the 6 optimization runs (scale 0, 1, 2, 3, 4 and 5), and figure 10 the evolution on the relative error on the parameter associated to each scale.

IV-4 Multiscale bases, multiresolution and regularization

When the data is noisy, the estimation error of approximation become [1, 9]

$$\|a_H - a\| \leq K_1(dist(z, \phi(Q_{ad}))H^{-s} + K_2 H^{\beta}. \tag{20}$$

So a_H may be far from a when H is sufficiently small. To stabilize the solution of inverse problem, the classical method is to use Tikonov's regularization [15], for example, replacing the objective function $J(a)$ by

$$J_1(a) = J(a) + \alpha \|\frac{da(x)}{dx}\|^2. \tag{21}$$

This function of course can be efficiently minimized using the multiresolution algorithm of paragraph 4.3. The numerical results corresponding to $\alpha = 10^{-6} J(a_{init})$ and 5% noisy data are shown on figure 11. We see that a stabilization is achieved to the price of less accurate fit to the true parameter value.

The use of multiscale basis and/or of multiresolution algorithm leads naturally to two other types of regularization:

If we use a multiscale basis, we can express the smoothness of a function by the decay of the coefficient in the expansion. So we can replace $J(a)$ by [8]

$$J_2(a) = J(a) + \sum_j \alpha_j \sum_i (c_i^j)^2 \tag{22}$$

Hence the regularization is obtained by limiting the amplitude of the small scale oscillations of a_H (compare with the usual regularization (21), where all scales are affected !) We refer to [8] for numerical results for this approach.

With the procedure of multiresolution, a very simple type of regularization (corresponding to the limit case of the equation (22) with $\alpha_j = 0, j = 0, ..., m$ and $\alpha_j = \infty$, $j > m$) can be performed, just by stopping at a reasonable scale during the multiresolution procedure. Different regularizations

can be obtained using different multiscale bases. For example, it is probably interesting to use some regular multiscale basis as Meyer's basis [14].

The figure 12 and figure 13 show the parameters obtained at different scales for 1% noise and for 5% noise respectively. As the noise increases, the oscillation increases also: hence we should stop the procedure of optimization at an adequate scale, i.e. regularize the solution. For example, we can stop at $4th$ scale (16 numbers) for 1% noise and at $3rd$ (8 numbers) for 5%. We remark that the solutions until $3th$ scale are the same with 5% noise or without noise (figure 9, 12, 13).

V Conclusion

We have studied numerically the use of a multiresolution approach for the inverse problem in a 1-D elliptic equation. It has been shown that the methodology of multiresolution is well-suited to solve this ill-posed nonlinear problem. The advantages of this method are:

- The final solution is independent of the choice of the initial parameters;
- Some local minima can be avoided;
- A very fast convergence is achieved;
- It leads naturally to the use of new types of regularizations which are likely to perturb less the low-frequency components of the optimal solution.

The methodology proposed in this paper is very general. It has been also used for the identification of the conductivity coefficient in a parabolical equation [8], and for the identification the relative permeabilities and capillary pressure [6]. We believe that this method will also prove to be powerful for more complicated inverse problems.

Acknowledgements

I am greatly indebted to Professor Guy Chavent for many helpful conversations.

Bibliography

[1] J. P. Aubin. *Approximation of Elliptic Boundary-Value Problems.* Wiley, New York, 1972.

[2] H. T. Banks and K. Kunisch. *Estimation Techniques for Distributed Parameter Systems.* Birkhauser, Boston ; Basel ; Berlin, 1989.

[3] A. Bensoussan, J. L. Lions, and G. Papanicolaou. *Asymptotic Analysis For Periodic Structures.* North-Holland, Amsterdam, 1978.

[4] A. Brandt. Multi-level Adaptive Solutions to Boundary Value Problems. *Math. Comp.*, 13:333–390, 1977.

[5] W. Briggs. *A Multigrid Tutorial.* Siam, Philadelphia, 1987.

[6] C. Chardaire, G. Chavent, J. Jaffré, and J. Liu. Multiscale representation for the simultaneous estimation of relative permeabilities and capillary pressure. In *SPE fall meeting*, News Orleans, USA, Sept, 1990.

[7] G. Chavent. A nonlinear least-square theory for inverse problems. In *Inverse Methods in Action.* Springer, 1990.

[8] G. Chavent and J. Liu. Multiscale parametrization for the estimation of a diffusion coefficient in elliptic and parabolic problems. In *5th IFAC Symposium on Control of Distributed Parameter Systems*, Perpignan, France, June, 1989.

[9] P.G. Ciarlet. *The Finite Element Method of Elliptic Problems.* North Holland, Amsterdam, 1978.

[10] R. S. Falk. Approximation of Inverse Problems. In *Inverse Problems in Partial Differential Equations*, pages 5–14, Philadelphia, 1988. SIAM.

[11] IMSL groupe. *IMSL Library Reference Manual - Version 10*, 1987.

[12] K. Kunisch and L. W. White. Identifiability under approximation for an elliptic boundary value problem. *SIAM J. Control and Optim.*, 25:279–297, 1987.

[13] S. G. Mallat. Multiresolution Approximation and Wavelet Orthonormal Bases of L^2. *Trans. Amer. Math. Soc.*, Jun 1977.

[14] Y. Meyer. *Ondelettes et Opérateurs.* Hermann, Paris, 1990.

[15] A. N. Tikonov and V. Y. Arsenin. *Solution of Ill-posed Problems.* Wiley, New York, 1977.

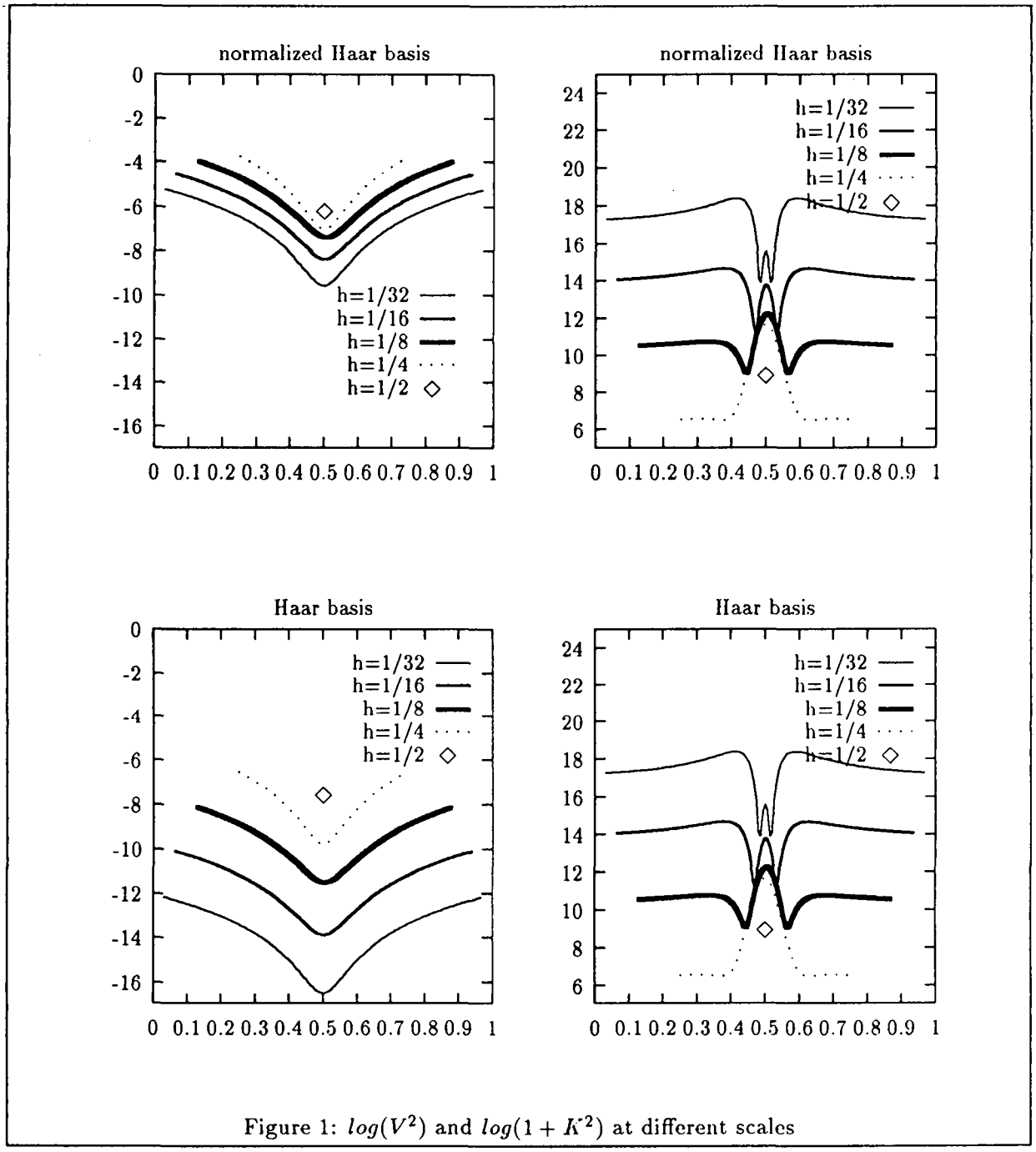

Figure 1: $log(V^2)$ and $log(1 + K^2)$ at different scales

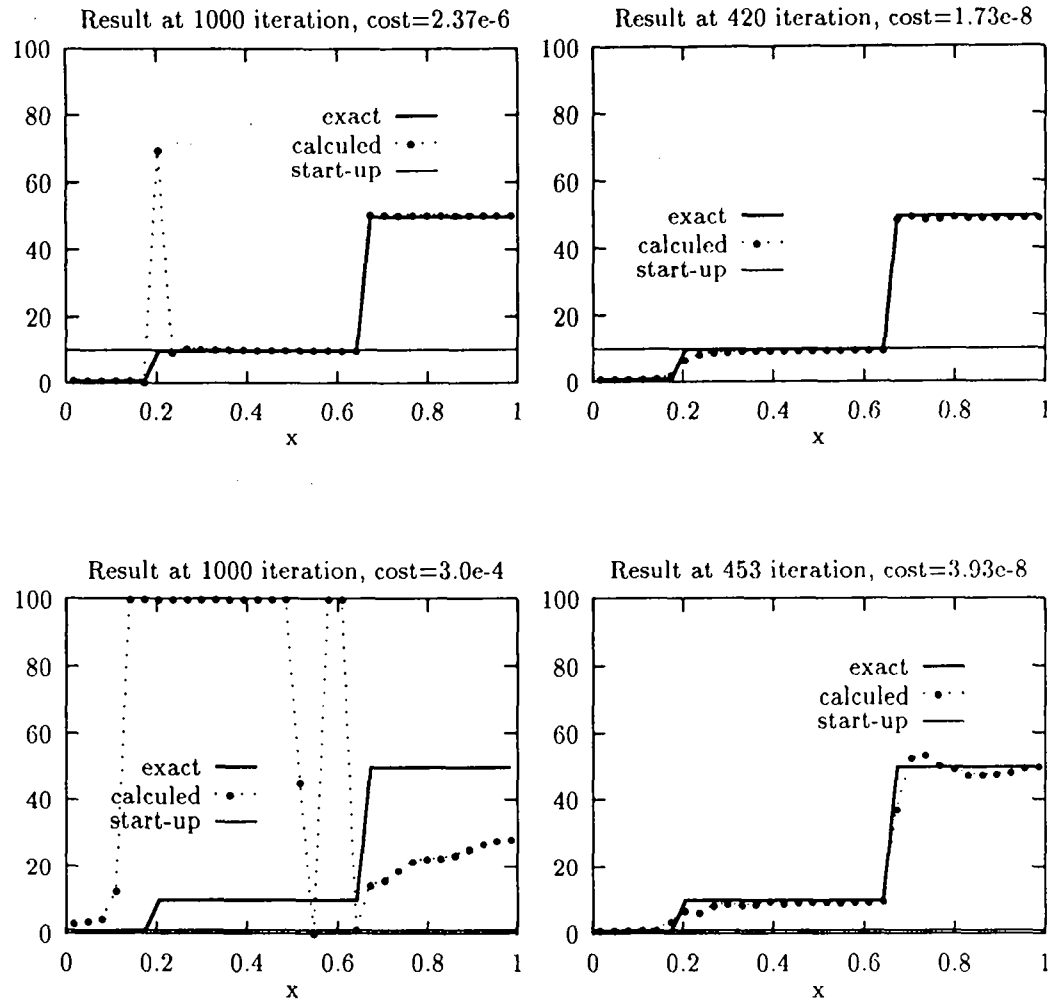

Figure 2: The comparison of the final results of minimisation for different initializations (bottom $a_{init} = 1$, top $a_{init} = 10$) and for different parametrizations of the unknown parameter (left: local basis, right: Haar basis). The bound constraint [0.1,100] was used with the local basis and no constraint was used with Haar basis.

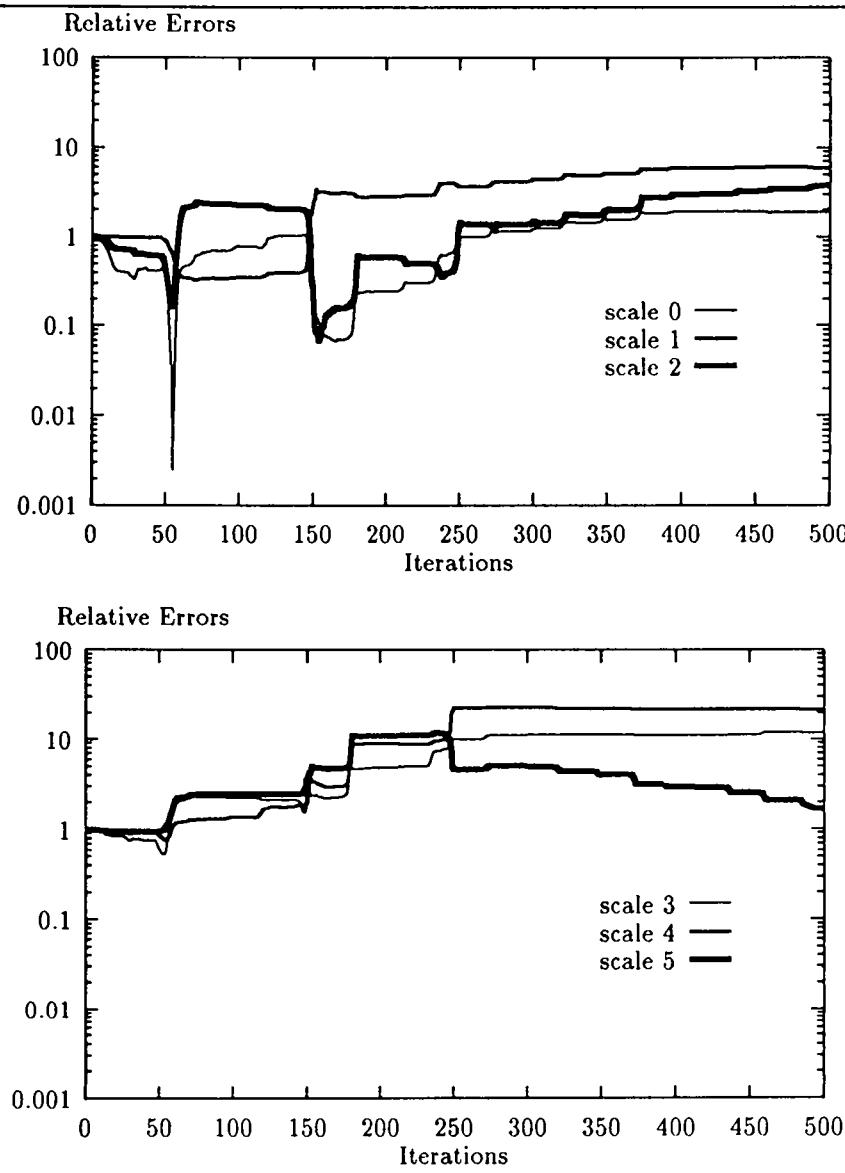

Figure 3: The evolution of relative errors on different scales for parameter $a(x)$ in L^2 during the optimization with the local basis, $a_{init} = 1$ and bound constraint= [0.1,100]

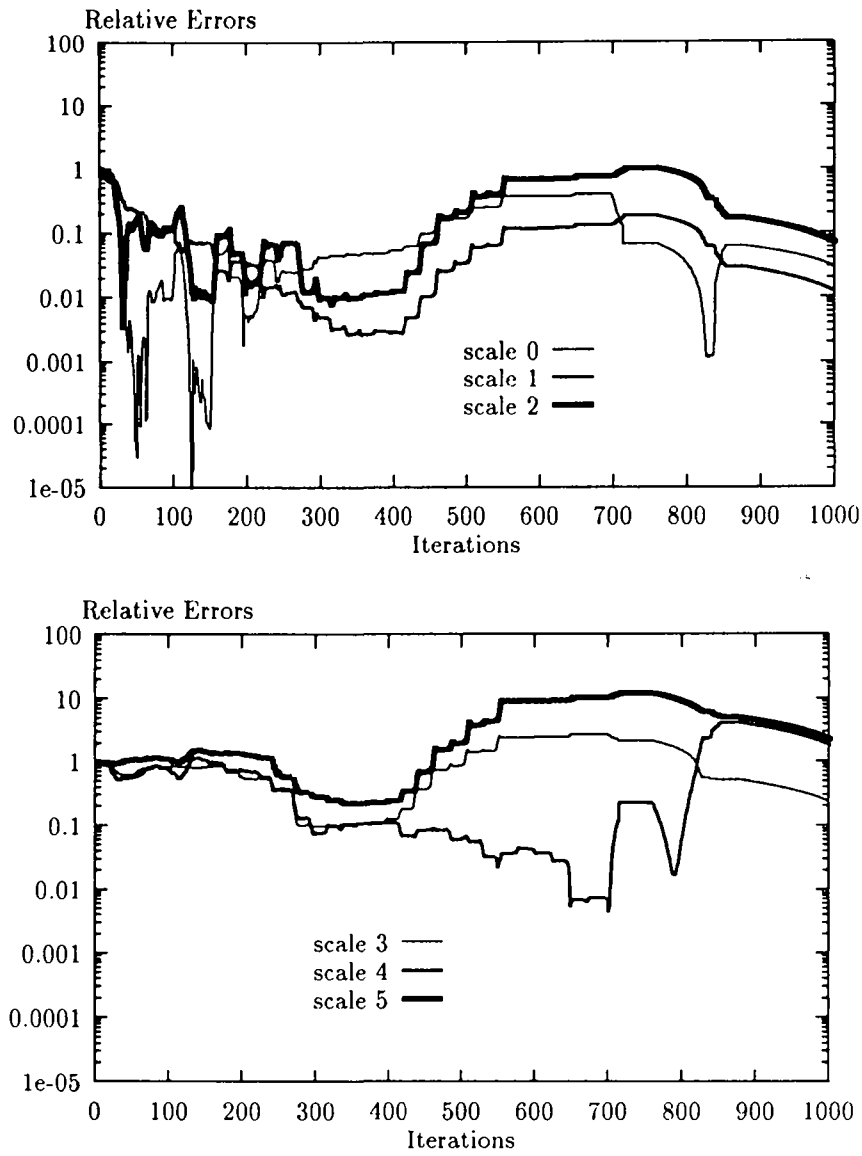

Figure 4: The evolution of relative errors on different scales for parameter $a(x)$ in L^2 during the optimization with the local basis, $a_{init} = 10$ and bound constraint=[0.1:100].

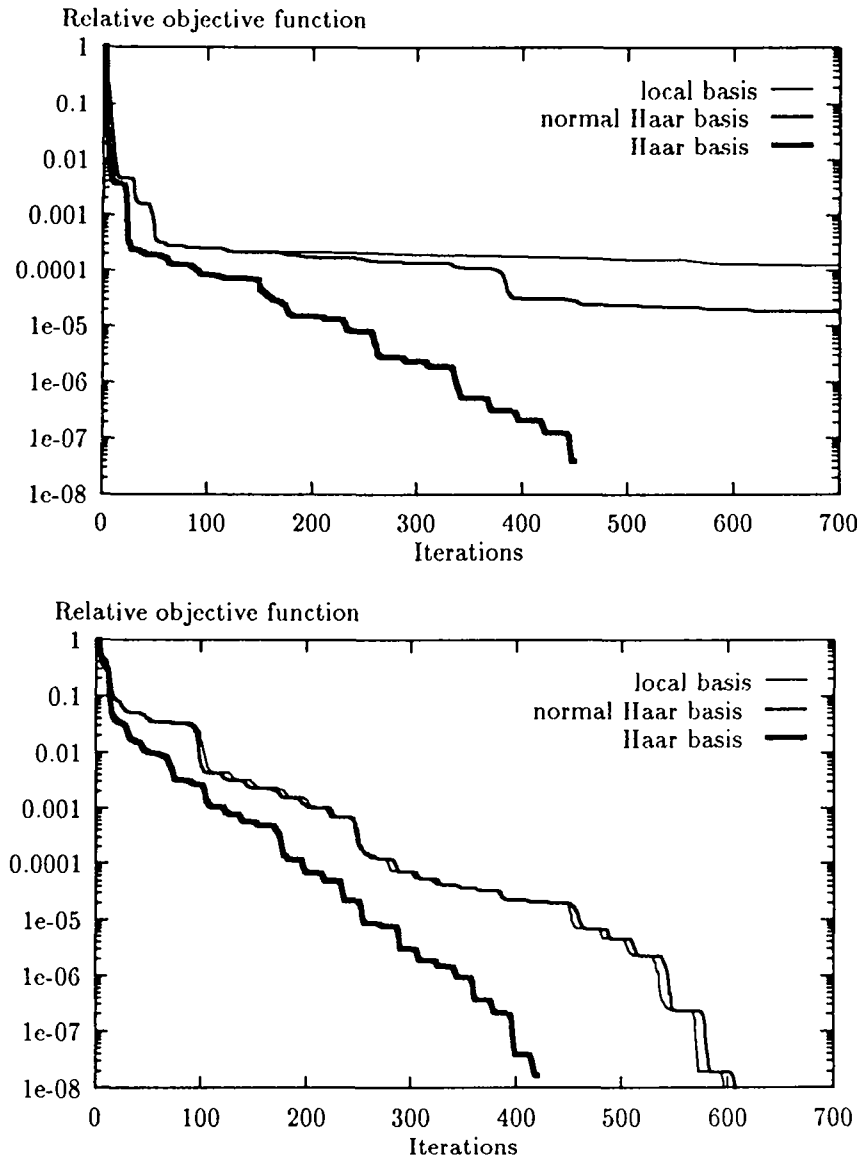

Figure 5: Convergence of the objective function obtained with local, normal Haar and Haar bases for $a_{init} = 1$ (top) and $a_{init} = 10$ (bottom) (no constraint was used).

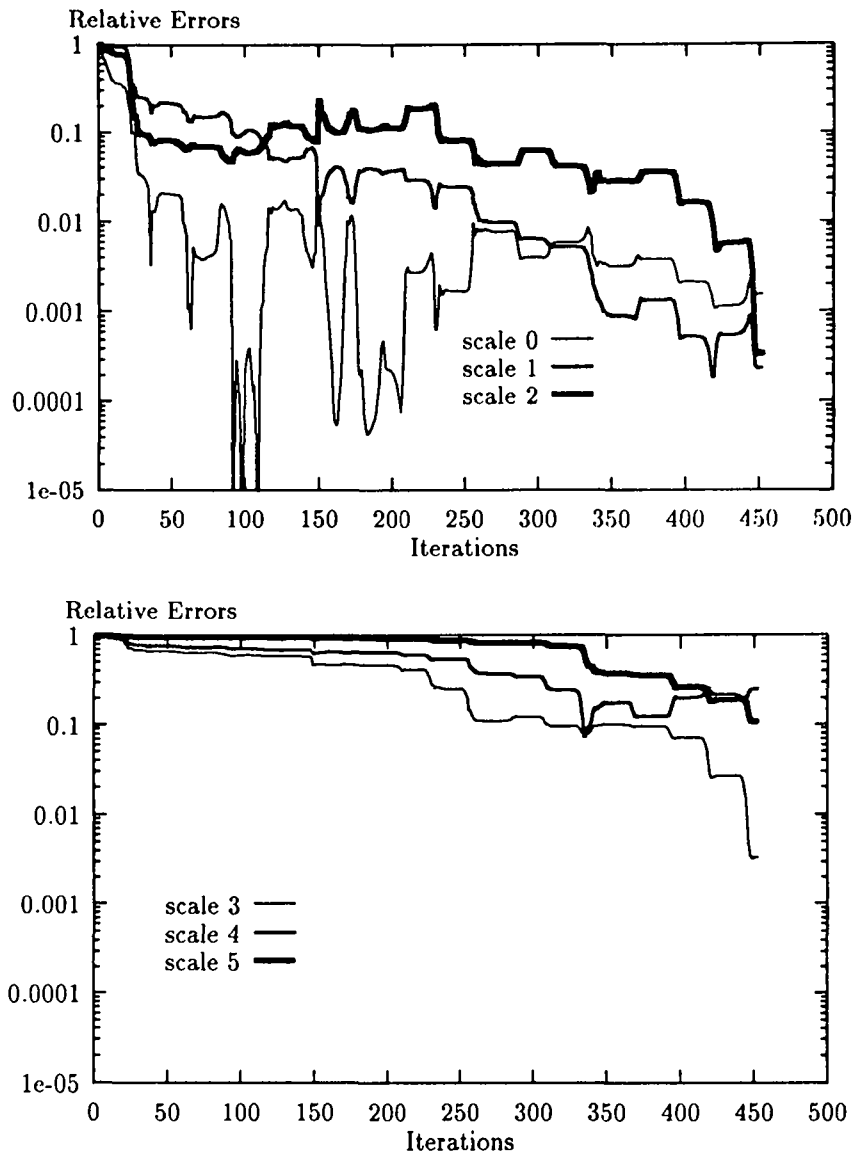

Figure 6: The evolution of relative errors on different scales for parameter $a(x)$ in L^2 during the optimization with the Haar basis and $a_{init} = 1$.

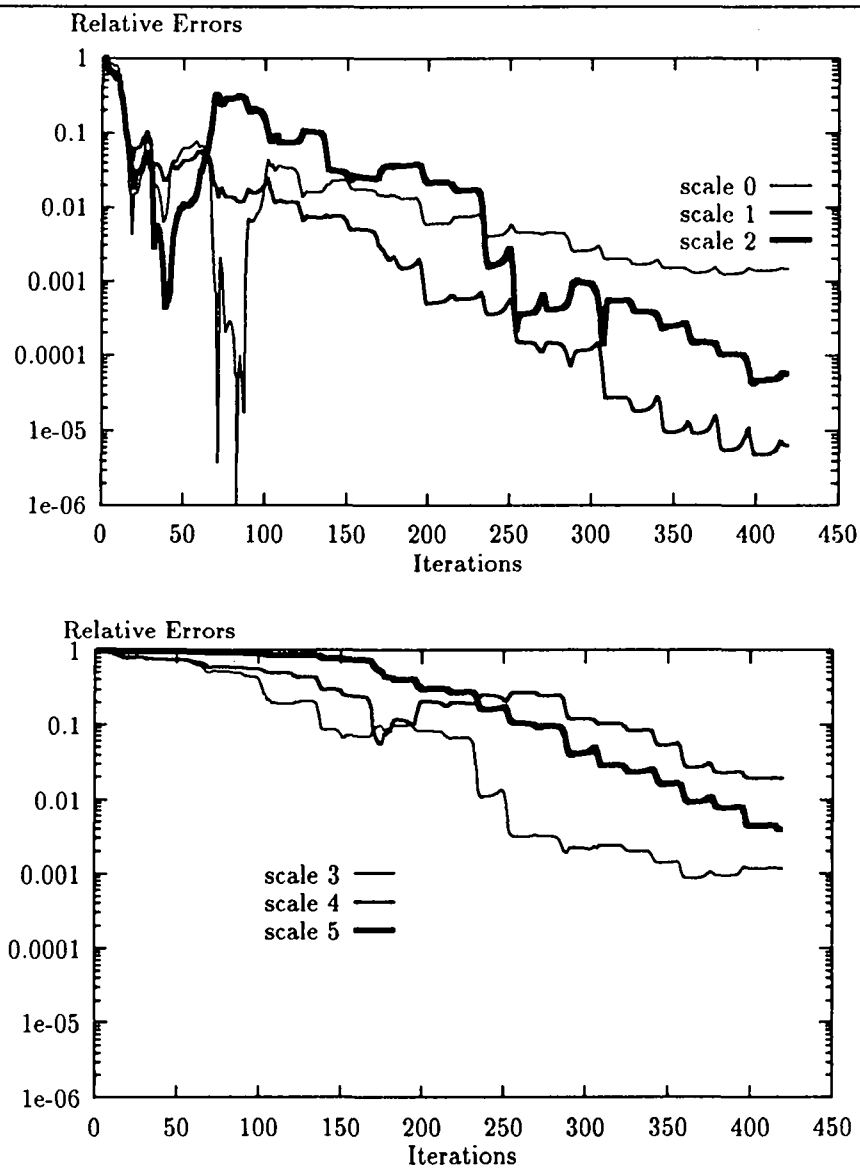

Figure 7: The evolution of relative errors on different scales for parameter $a(x)$ in L^2 during the optimization using the Haar basis with $a_{init} = 10$.

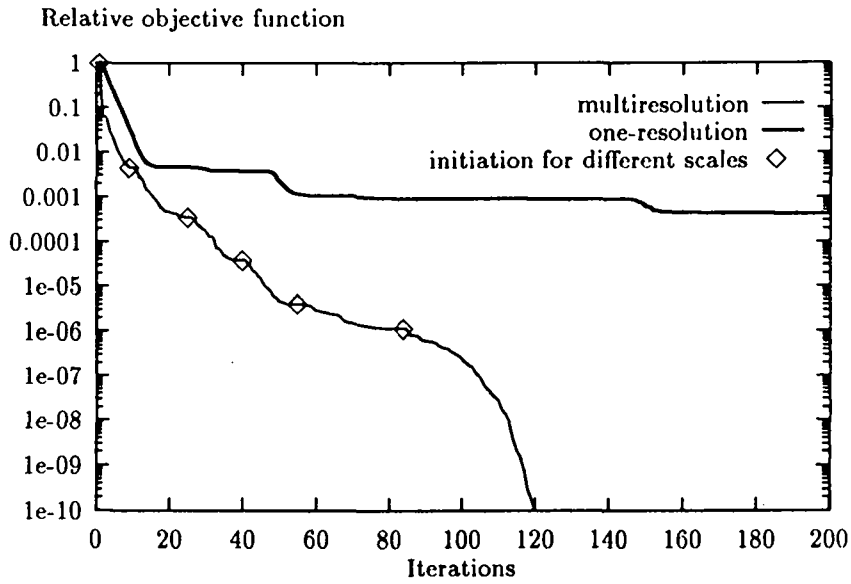

Figure 8: Convergence of the objective function obtained with single- and multi- resolution (the local basis and $a_{init} = 1$ were used in both cases).

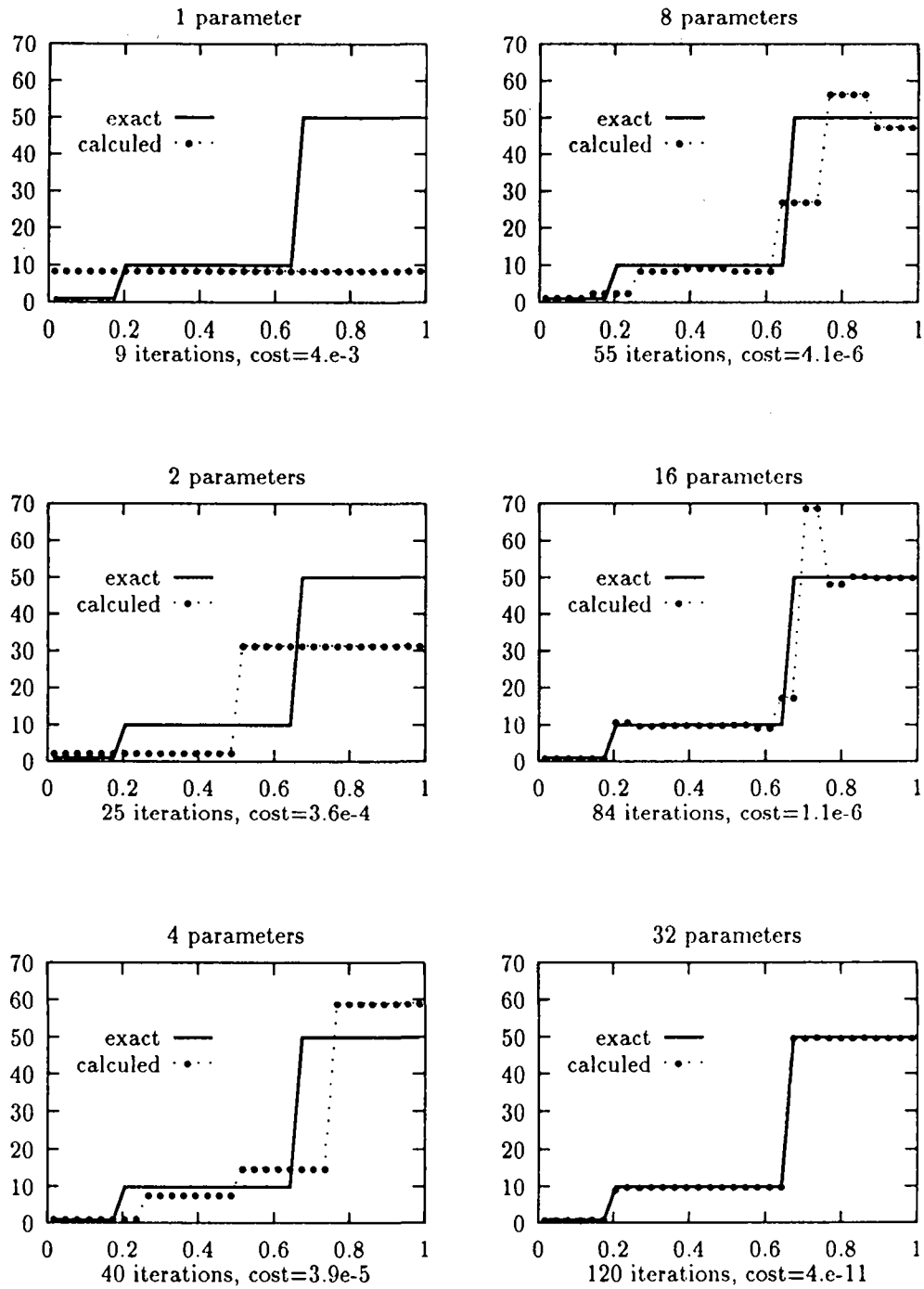

Figure 9: The parameter obtained at the end of each step (scale level) of the multiresolution method without noise

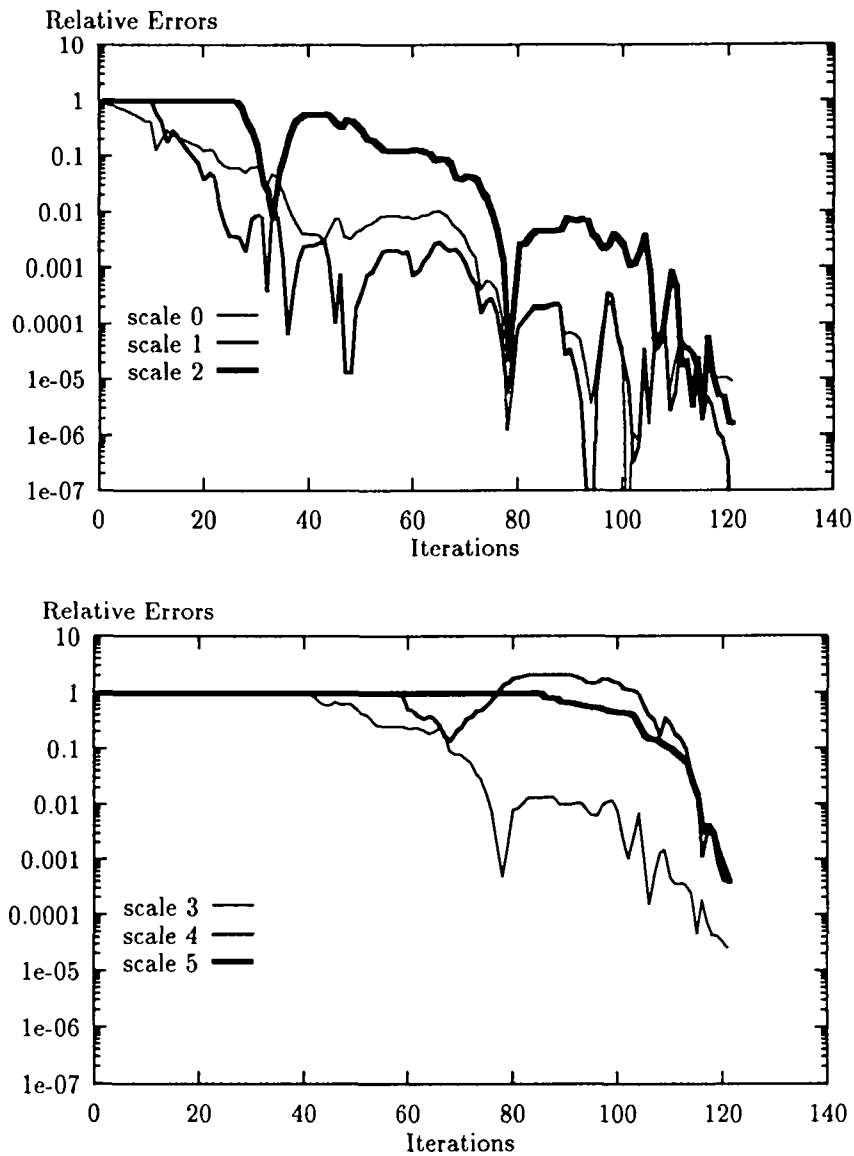

Figure 10: The evolution of relative errors on different scales for parameter $a(x)$ in L^2 during the optimization with $a_{init} = 1$ and bound constraint [0.1:100] using multiresolution

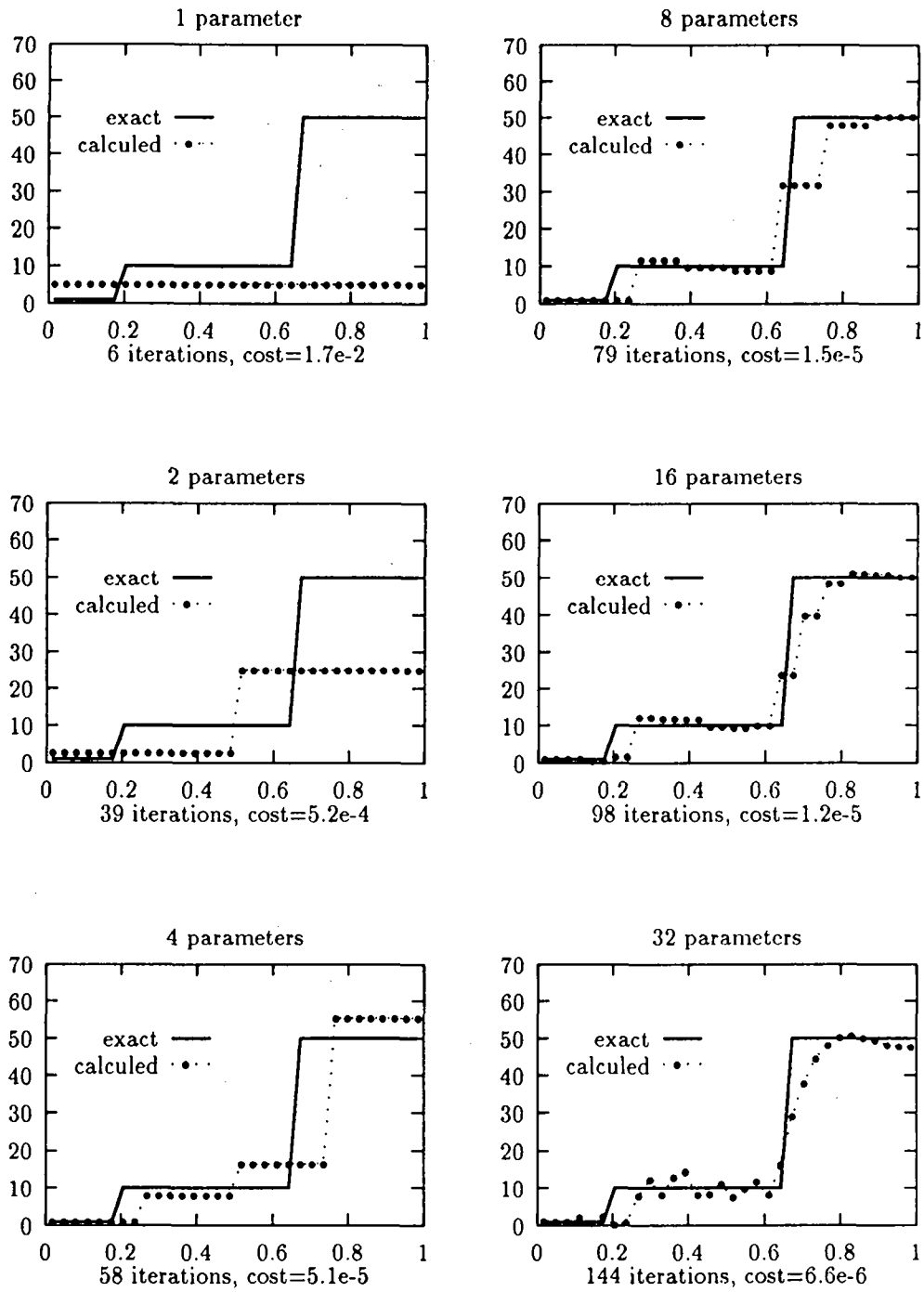

Figure 11: The parameter obtained at the end of each step (scale level) of the multiresolution method applied to Tikonov's regularized problem and data with 5% noise

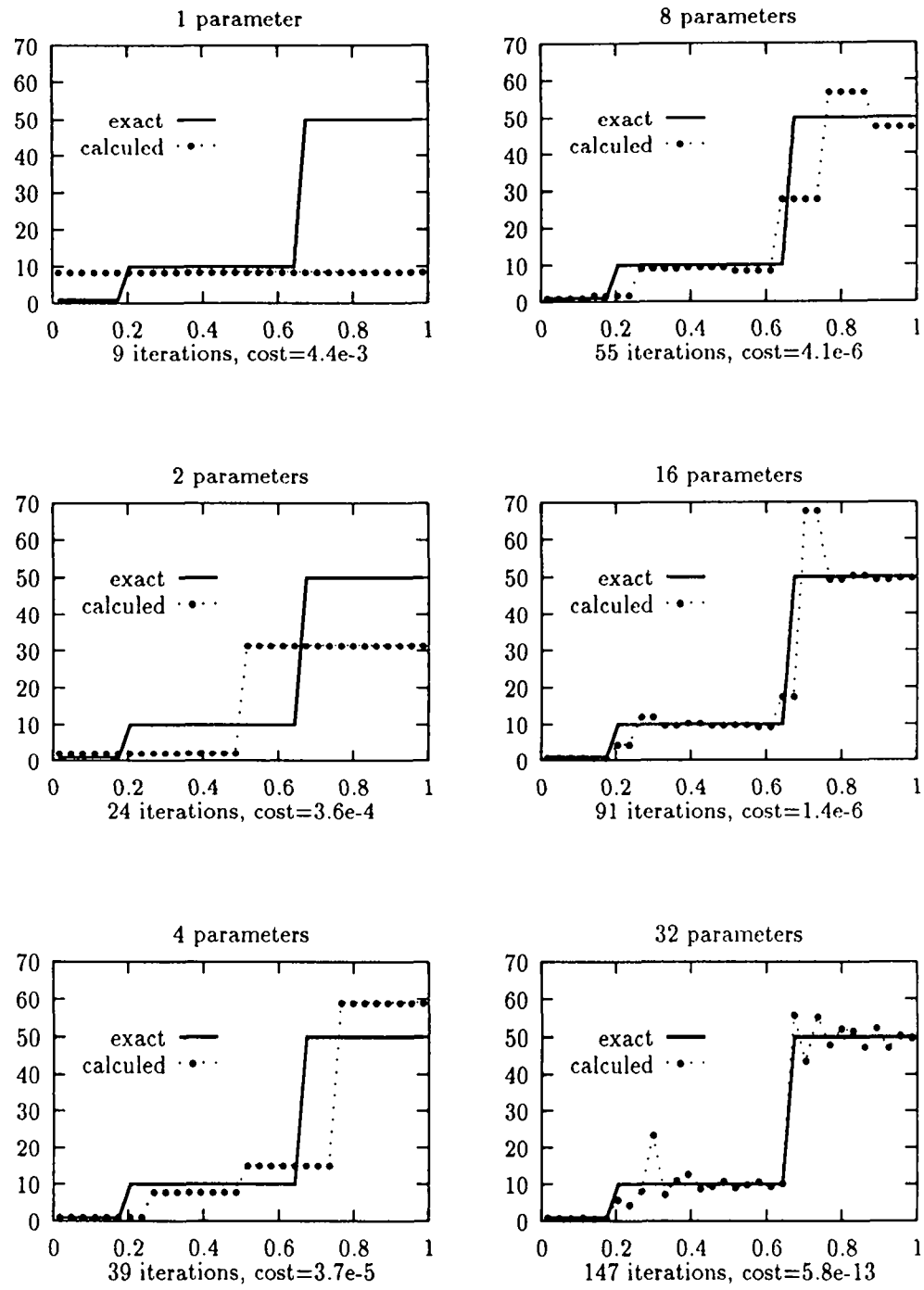

Figure 12: The parameter obtained at the end of each step (scale level) of the multiresolution method applied to the unregularized problem and data with 1% noise

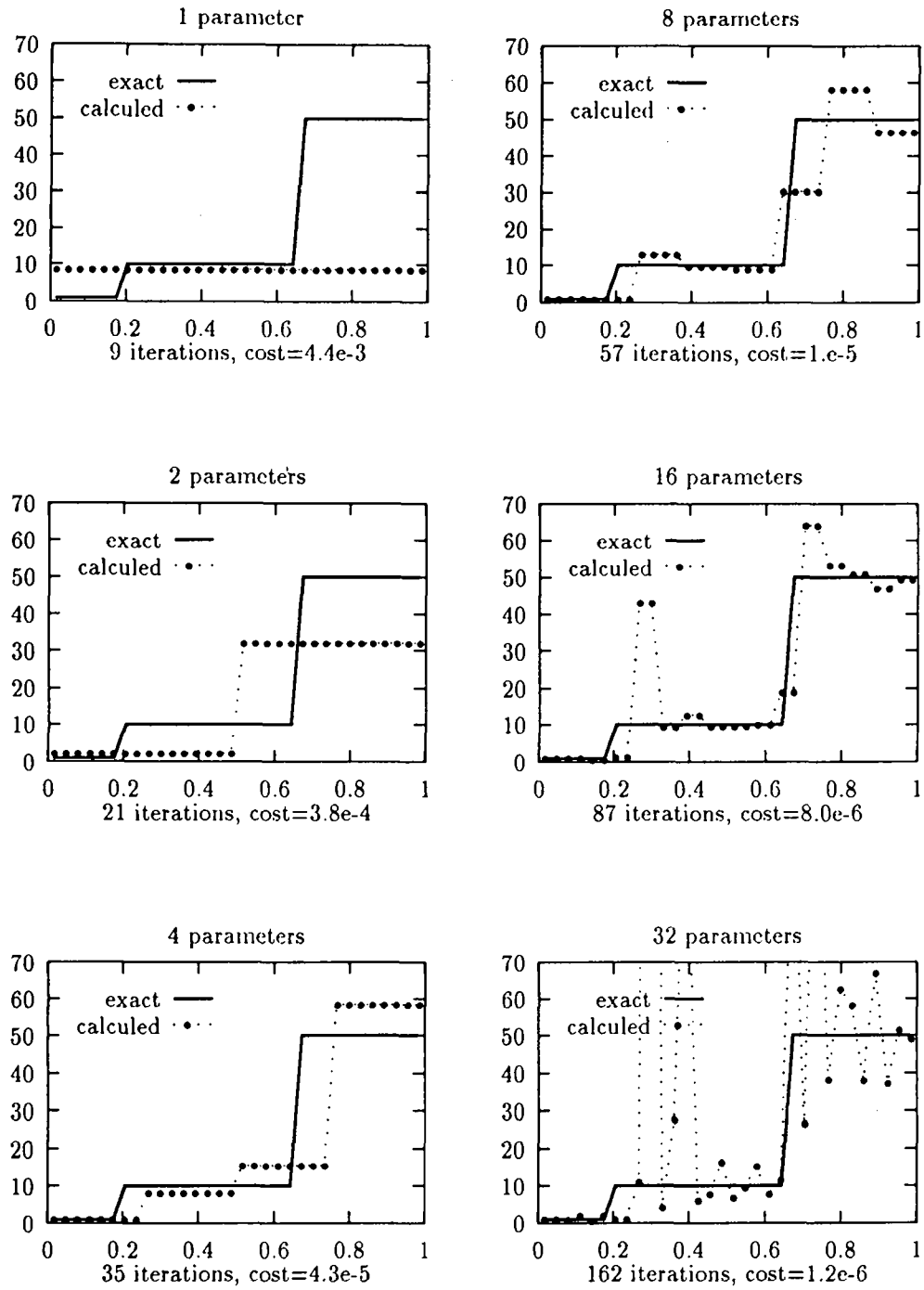

Figure 13: The parameter obtained at the end of each step (scale level) of the multiresolution method applied to the unregularized problem and data with 5% noise

Imprimé en France
par
. l'Institut National de Recherche en Informatique et en Automatique

ISSN 0249-6399